Stabilizing Superionic-Conducting Structures via Mixed-Anion Solid Solutions of Monocarba-*closo*-borate Salts

Wan Si Tang,*,†,‡ Koji Yoshida,§ Alexei V. Soloninin,‖ Roman V. Skoryunov,‖ Olga A. Babanova,‖ Alexander V. Skripov,‖ Mirjana Dimitrievska,†,⊥ Vitalie Stavila,# Shin-ichi Orimo,*,§,∇ and Terrence J. Udovic*,†

†NIST Center for Neutron Research, National Institute of Standards and Technology, Gaithersburg, Maryland 20899-6102, United States

‡Department of Materials Science and Engineering, University of Maryland, College Park, Maryland 20742-2115, United States

§Institute for Materials Research, Tohoku University, Sendai 980-8577, Japan

‖Institute of Metal Physics, Ural Branch of the Russian Academy of Sciences, Ekaterinburg 620990, Russia

⊥National Renewable Energy Laboratory, Golden, Colorado 80401, United States

#Energy Nanomaterials, Sandia National Laboratories, Livermore, California 94551, United States

∇WPI-Advanced Institute for Materials Research, Tohoku University, Sendai 980-8577, Japan

Ⓢ *Supporting Information*

ABSTRACT: Solid lithium and sodium *closo*-polyborate-based salts are capable of superionic conductivities surpassing even liquid electrolytes, but often only at above-ambient temperatures where their entropically driven disordered phases become stabilized. Here we show by X-ray diffraction, quasielastic neutron scattering, differential scanning calorimetry, NMR, and AC impedance measurements that by introducing "geometric frustration" via the mixing of two different *closo*-polyborate anions, namely, 1-$CB_9H_{10}^-$ and $CB_{11}H_{12}^-$, to form solid-solution anion-alloy salts of lithium or sodium, we can successfully suppress the formation of possible ordered phases in favor of disordered, fast-ion-conducting alloy phases over a broad temperature range from subambient to high temperatures. This result exemplifies an important advancement for

further improving on the remarkable conductive properties generally displayed by this class of materials and represents a practical strategy for creating tailored, ambient-temperature, solid, superionic conductors for a variety of upcoming all-solid-state energy devices of the future.
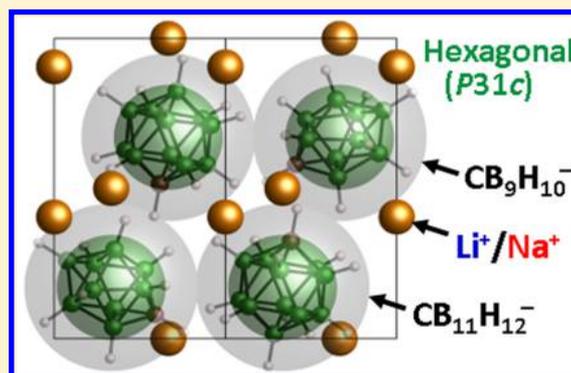
We have previously shown that the broad class of *closo*-polyborate salt compounds containing lithium and sodium cations routinely exhibit entropy-driven order−disorder transitions to become impressive superionic conductors.[1−4] The most spectacular ones to date are based on the more weakly coordinating monovalent $CB_{11}H_{12}^-$ and 1-$CB_9H_{10}^-$ anions. For example, $NaCB_9H_{10}$ displays a room-temperature Na+ conductivity of about 0.03 S cm−1,[4] which well surpasses that of any known polycrystalline Na or Li competitors,[5−7] including many liquid Na+ or Li+ electrolytes.[8−10] The ionic saltlike nature of all these compounds guarantees negligible electronic conductivity. Moreover, the overly large cagelike anions, although orientationally extremely mobile, remain translationally rigid within high-symmetry [face-centered-cubic (fcc), body-centered-cubic (bcc), or hexagonal],

disordered, cation-vacancy-rich lattices, and their pseudoaromatic nature[11] leads to high chemical and electrochemical stability. All these observed disordered symmetries exhibit superionic conductivities, and although it is believed from purely geometric arguments that the bcc lattice is relatively superior for cation diffusion,[12] the more subtle effects of lattice structure on conductivity for these types of compounds seem to be overwhelmed by other factors such as the cooperative effects of anion reorientational motions on cation translations.
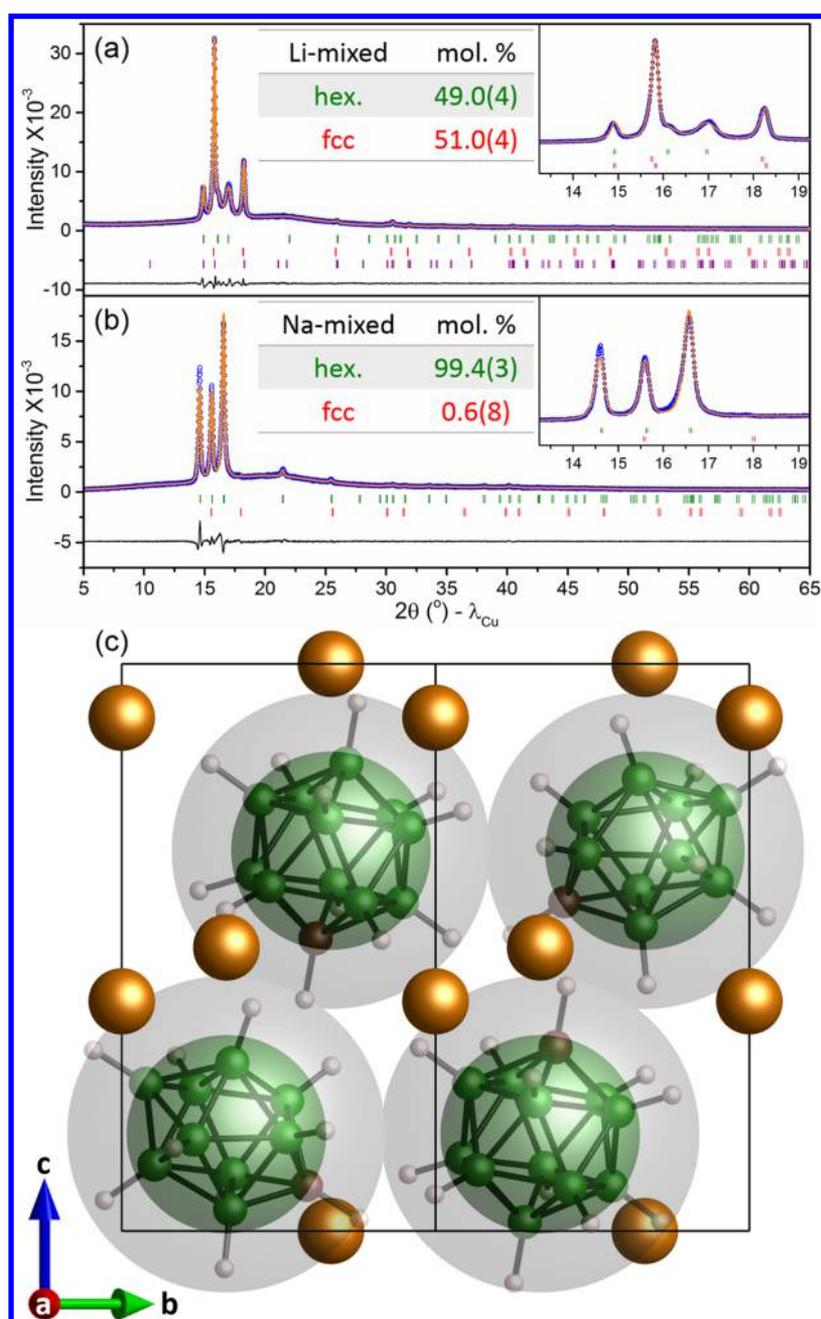
Figure 1. Room-temperature XRPD data [experimental (blue circles), fitted (orange line), and difference (black line) patterns] for solution-dried (a) $Li_2(CB_9H_{10})(CB_{11}H_{12})$ and (b) $Na_2(CB_9H_{10})(CB_{11}H_{12})$. Vertical green and red bars indicate the positions of Bragg peaks for the high-T hexagonal and fcc phases, respectively. The refined unit cell parameters for the Li-mixed sample are $a = 6.8589(5)$ Å, $c = 11.0116(11)$ Å, and $V = 448.64(6)$ Å^3 for the hexagonal structure; $a = 9.7541(7)$ Å and $V = 928.03(11)$ Å^3 for the fcc structure ($\chi^2 = 2.40$; $R_p = 0.110$; $R_{wp} = 0.0965$). Refinement indicated an additional disordered phase (purple bars) indexed by profile matching to a probable hexagonal unit cell with parameters $a = 6.86$ Å and $c = 16.85$ Å. The refined unit cell parameters for the Na-mixed sample are $a = 6.9905(11)$ Å, $c = 11.3390(17)$ Å, and $V = 479.88(13)$ Å^3 for the hexagonal structure; $a = 9.855(3)$ Å and $V = 957.1(5)$ Å^3 for the fcc structure ($\chi^2 = 3.19$; $R_p = 0.156$; $R_{wp} = 0.132$). (c) The disordered hexagonal structure with orange Li^+/Na^+ cation positions and large green (B/C atoms) and gray (H atoms) spheres denoting the diffraction-average spherical shells of scattering from the orientationally disordered $CB_9H_{10}^-$ and $CB_{11}H_{12}^-$ anions (superimposed).

To make these materials more relevant for near-ambient-temperature device technologies, we need strategies for lowering (well below room temperature) or completely eliminating the transition temperature to the structurally disordered phases responsible for superionic conduction. This can be potentially accomplished in various ways. One obvious approach is to chemically modify the anions. A good example is the replacement of one apical boron atom of $B_{10}H_{10}^{2-}$ with

carbon to form $1\text{-}CB_9H_{10}^-$ anions. The resulting $NaCB_9H_{10}$ salt possesses a lower transition temperature and a higher conductivity than $Na_2B_{10}H_{10}$.[2,4] More recently, we successfully demonstrated a second approach: that the disordered structures, and thus superionic conductivity, for a variety of *closo*-polyborate salts could indeed typically be stabilized at room temperature and below by crystallite nanosizing/disordering via mechanical milling.[13]

Here we demonstrate a third approach to stabilize disordered superionic structures well below room temperature without the need for mechanical milling, i.e., by synthesizing mixed-*closo*-polyborate-anion compounds from solutions. In particular, we formed $Li_2(CB_9H_{10})(CB_{11}H_{12})$ and $Na_2(CB_9H_{10})(CB_{11}H_{12})$ compound mixtures by drying aqueous solutions with equimolar amounts of either $LiCB_9H_{10} + LiCB_{11}H_{12}$ or $NaCB_9H_{10} + NaCB_{11}H_{12}$. Figure 1 displays the room-temperature X-ray powder diffraction (XRPD) patterns of the resulting precipitated mixtures after final vacuum drying steps overnight at 473 K. Rietveld refinement results for $Li_2(CB_9H_{10})(CB_{11}H_{12})$ confirm the formation of two equally prevalent disordered phases, one hexagonal (but with a slightly larger unit cell) like that found for pristine superionic $LiCB_9H_{10}$ above ≈350 K[4] and another fcc (but with a slightly smaller unit cell) like that found for pristine superionic $LiCB_{11}H_{12}$ above ≈395 K.[3] The different phases are due to either similar-energy disordered polymorphs, which is possible for *closo*-polyborates,[1,3] or incomplete homogenization yielding two mixture fractions, one that is slightly CB_9H_{10}-rich (hexagonal) and one that is slightly $CB_{11}H_{12}$-rich (fcc). The larger hexagonal lattice is consistent with the substitution of larger $CB_{11}H_{12}^-$ anions for smaller $CB_9H_{10}^-$ anions in the $LiCB_9H_{10}$-like disordered hexagonal structure, and the smaller fcc lattice is consistent with the substitution of smaller $CB_9H_{10}^-$ anions for larger $CB_{11}H_{12}^-$ anions in the $LiCB_{11}H_{12}$-like disordered fcc structure. In addition, a very minor fraction of a third disordered phase seems to be present, similar to the additional hexagonal (h2) polymorph previously observed at 428 K for $NaCB_{11}H_{12}$.[3] We stress that these different hexagonal and fcc disordered structures have been shown to be superionic for the single-anion analogs.[3,4]

For $Na_2(CB_9H_{10})(CB_{11}H_{12})$, Rietveld refinement results confirm the formation of a predominant disordered hexagonal phase (but with a slightly larger unit cell) like that found for pristine superionic $NaCB_9H_{10}$ above ≈310 K[4] (with a minute fraction of fcc phase also present). The larger lattice again is consistent with the substitution of larger $CB_{11}H_{12}^-$ anions for $CB_9H_{10}^-$ anions in the $NaCB_9H_{10}$-like disordered hexagonal structure. We point out that the relatively low scattering from the liquidlike sublattice of cations associated with both the Na- and Li-based disordered mixtures precluded us from determining the distribution and occupations of cation interstitial sites using XRPD data. This will require additional neutron powder diffraction studies with ^{11}B-enriched, deuterated samples, which are currently unavailable.

Differential scanning calorimetry (DSC) measurements for both mixtures cycled between 200 and 473 K (Figure S1 of the Supporting Information) displayed no obvious endothermic or exothermic phase transitions, indicating that the disordered solid-solution phases are stable at least within this temperature range.

Figure 2 shows NMR measurements of the ^1H spin–lattice relaxation rates R_1^H for $Li_2(CB_9H_{10})(CB_{11}H_{12})$ and $Na_2(CB_9H_{10})(CB_{11}H_{12})$. For comparison, this figure also includes the fitted $R_1^H(T)$ results[14] for the pristine $LiCB_{11}H_{12}$ and $NaCB_{11}H_{12}$ compounds undergoing their order–disorder phase transitions near 384 and 376 K, respectively. Figure 2 indicates that both Li- and Na-based mixtures retain high anion reorientational mobilities down to low temperatures because of the suppression of transitions to ordered phases. Indeed, the $R_1^H(T)$ maximum (corresponding to the H jump rate of ≈10^8 s^{-1}) is observed near 230 K for $Li_2(CB_9H_{10})(CB_{11}H_{12})$ and

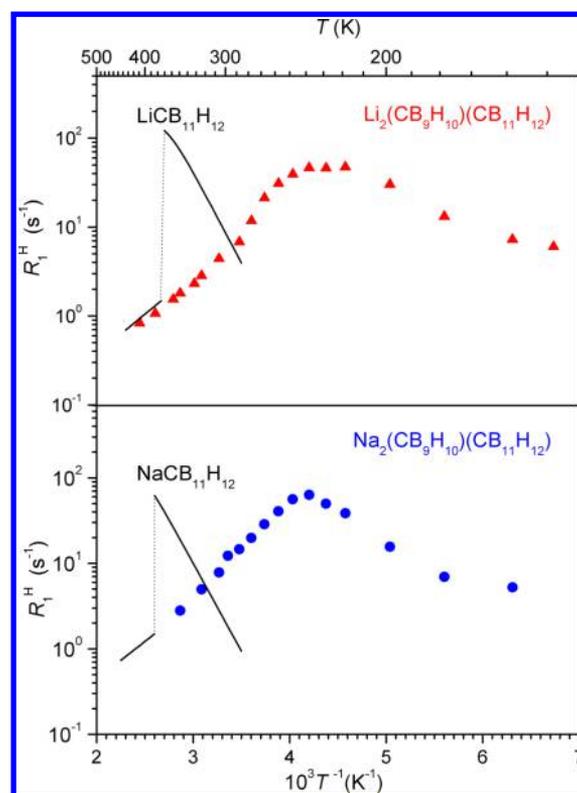**Figure 2.** Proton spin–lattice relaxation rates measured at 28 MHz versus inverse temperature for $Li_2(CB_9H_{10})(CB_{11}H_{12})$ and $Na_2(CB_9H_{10})(CB_{11}H_{12})$. The black lines show the fits to the proton spin–lattice relaxation rates at the same frequency for $LiCB_{11}H_{12}$ and $NaCB_{11}H_{12}$ from ref 14 undergoing their order–disorder phase transitions near 384 and 376 K, respectively.

near 220 K for $Na_2(CB_9H_{10})(CB_{11}H_{12})$. For both mixtures, room temperature corresponds to the high-T slope of the $R_1^H(T)$ peak (fast-motion limit), and a rough estimate of the H jump rate at 300 K gives 10^{10} s^{-1}. It is interesting to note that for both mixtures, the high-T slope of the relaxation rate peak looks like a continuation of the slope for the disordered phase of the corresponding $MCB_{11}H_{12}$ compound. The activation energies for reorientational motion estimated from the high-T slopes are 220 meV for $Li_2(CB_9H_{10})(CB_{11}H_{12})$ and 180 meV for $Na_2(CB_9H_{10})(CB_{11}H_{12})$, values close to the activation energies found for the disordered phases of both $LiCB_{11}H_{12}$ and $NaCB_{11}H_{12}$ (177 meV).[14] Moreover, the experimental $R_1^H(T)$ data for both mixtures indicate the presence of certain distributions of H jump rates. The characteristic signs of such distributions[15] include (i) the considerably smaller $R_1^H(T)$-peak amplitudes for the solid solutions compared to those for the pure component salts[14] and (ii) the steeper high-T slopes of the $R_1^H(T)$ peaks compared to the low-T slopes (see Figure 2). Distributions of reorientational jump rates are expected, because there are two types of anions, and their disordered local environments will vary from one anion to the next. While for $Na_2(CB_9H_{10})(CB_{11}H_{12})$ the proton spin–lattice relaxation is found to be single-exponential over the studied temperature range, deviations from the single-exponential relaxation are observed for $Li_2(CB_9H_{10})(CB_{11}H_{12})$ below 270 K. (In this range, Figure 2 shows the results of a single-exponential approximation.) This feature is likely related to the coexistence of two disordered phases (hexagonal and fcc), as indicated in Figure 1a. To probe the cation mobility, we have also measured

the ^{23}Na NMR spectra in $Na_2(CB_9H_{10})(CB_{11}H_{12})$ and found an extremely narrow ^{23}Na NMR line (0.4 kHz fwhm) at room temperature, indicating a fast, long-range diffusive motion of Na^+ cations with a jump rate exceeding at least $\approx 10^4$ s^{-1} (the lower limit from the ^{23}Na NMR spectral measurements).

In agreement with the NMR results, neutron-elastic-scattering fixed-window scans (FWSs) between 100 and 400 K for the Li and Na sample mixtures in Figure 3 also indicate
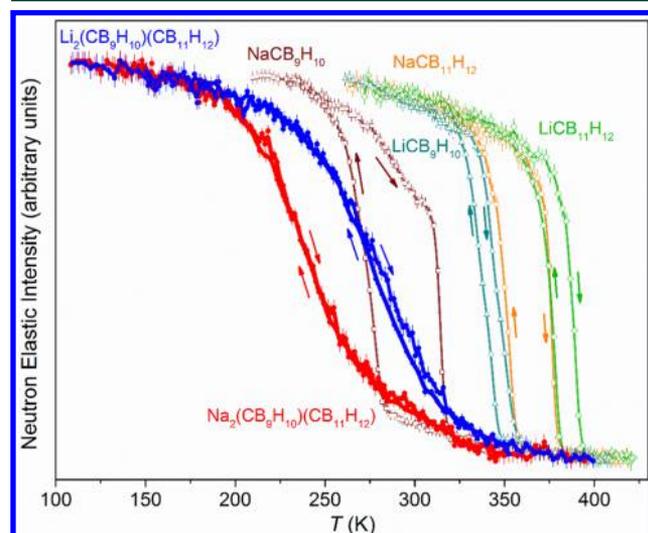

Figure 3. Neutron elastic-scattering FWSs for $Li_2(CB_9H_{10})$-$(CB_{11}H_{12})$ and $Na_2(CB_9H_{10})(CB_{11}H_{12})$ compared with those for the various single-anion component compounds, summed over detectors covering a Q range of 0.87−1.68 Å^{-1}. Arrows differentiate heating and cooling scans. For a reasonable qualitative comparison, the individual data sets were scaled so as to have similar minimum and maximum intensities.

highly mobile anion reorientational motions already approaching 10^8 jumps s^{-1} by around 240 and 210 K, respectively, as signaled by the onset of the drop in neutron elastic intensity near these temperatures. The jump rates attain the order of 10^{10} reorientational jumps s^{-1} by around 330 and 300 K, respectively, as the FWS intensities level off again. For comparison, the much sharper intensity changes for the FWSs for the pure component salts at higher temperatures mark the more abrupt hysteretic phase-change behaviors from relatively immobile anions in the lower-T ordered phases ($<10^8$ jumps s^{-1}) to significantly more mobile anions in the high-T disordered phases ($>10^{10}$ jumps s^{-1}). The high anion mobility seen for the anion mixtures by both NMR and FWSs is representative behavior of superionic-conducting disordered *closo*-polyborate phases.[3,4,14]

Figure 4 shows the T-dependent ionic conductivity for $Li_2(CB_9H_{10})(CB_{11}H_{12})$ and $Na_2(CB_9H_{10})(CB_{11}H_{12})$ compared with that for the component compounds.[3,4] As for the component compounds,[3,4] the complex impedance plots of the solid solutions in Figure S2 represent purely ionic conductors. The $Li_2(CB_9H_{10})(CB_{11}H_{12})$ conductivity seems to match that for disordered $LiCB_9H_{10}$ (ref 4) and $Li_{10}GeP_2S_{12}$ (ref 5) at 350 K (≈ 0.04 S cm^{-1}) and above, remaining somewhat lower than that for disordered $LiCB_{11}H_{12}$ (ref 3) above 380 K. Below 350 K, the $Li_2(CB_9H_{10})(CB_{11}H_{12})$ conductivity decreases below that of $Li_{10}GeP_2S_{12}$ to ≈ 4 μS cm^{-1} by 243 K. The $Na_2(CB_9H_{10})(CB_{11}H_{12})$ conductivity is much more impressive, seemingly even better than
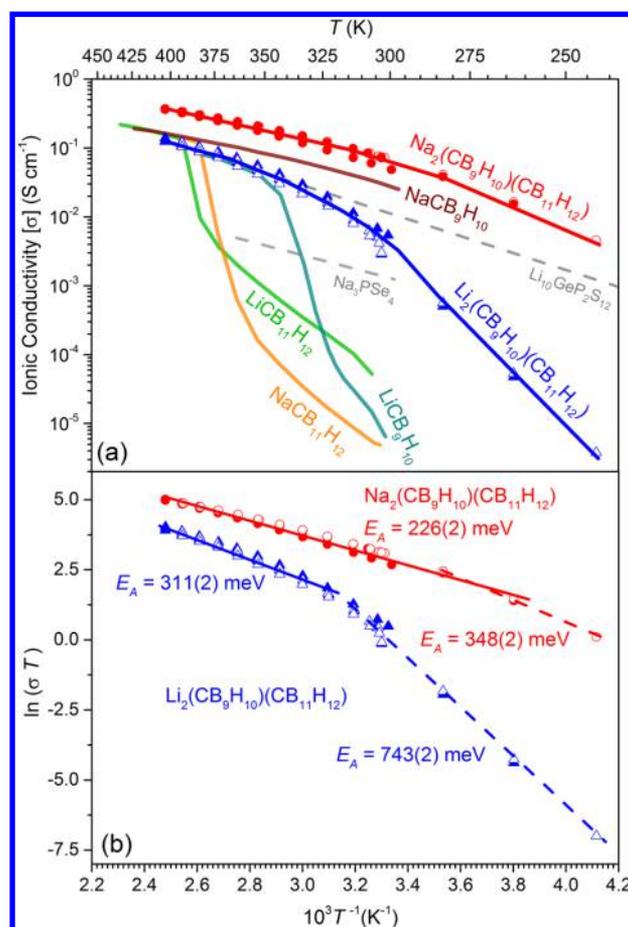

Figure 4. (a) Temperature dependences of the ionic conductivities (σ) for solution-dried, cold-pressed $Li_2(CB_9H_{10})(CB_{11}H_{12})$ and $Na_2(CB_9H_{10})(CB_{11}H_{12})$ using Li and Au electrodes, respectively, compared with those for the single-anion compounds[3,4] and the closest-performing competitors, $Li_{10}GeP_2S_{12}$ and Na_3PSe_4,[5,6] and (b) $\ln(\sigma T)$ vs T^{-1} and resulting fitted activation energies for the two mixed compounds. Closed and open symbols denote heating and cooling cycles, respectively.

disordered $NaCB_9H_{10}$ and $NaCB_{11}H_{12}$ at all temperatures,[3,4] and decreasing much less rapidly with temperature, from ≈ 0.07 S cm^{-1} at 300 K to ≈ 5 mS cm^{-1} at 243 K. This disordered solid-solution Na^+ conductor displays conductivity substantially higher than that of any known solid Na^+ or Li^+ conductor. Indeed, a 300 K comparison in Figure 4 shows that it is roughly 50× more conductive than its closest Na^+ competitor, Na_3PSe_4,[6] and around 7× better than $Li_{10}GeP_2S_{12}$.[5] The relatively larger cell constants, higher anion mobility, and potentially weaker cation−anion interactions for $Na_2(CB_9H_{10})$-$(CB_{11}H_{12})$ [compared to $Li_2(CB_9H_{10})(CB_{11}H_{12})$] likely all contribute to its unmatched conductivity.

The conductivity barriers estimated in Figure 4 [311(2) meV and 226(2) meV for Li^+ and Na^+, respectively] above room temperature, are in general agreement with those for the single-anion compounds.[3,4] The apparent changes in the overall barriers at subambient temperatures [to 743(2) and 348(2) meV, respectively] signal changes in the rate-limiting steps. If the highly reorientationally mobile anions are enabling a reduced conductivity barrier at higher temperatures via a cooperative dynamical effect with the diffusing cations, a higher barrier emerging with decreasing temperatures may be

indicating their reducing influence due to decreasing mobility. Further insights still await molecular dynamics computations.

The combined experimental results above suggest that mixing anions of slightly different geometric "flavors" such as $CB_9H_{10}^-$ (ellipsoidal) and $CB_{11}H_{12}^-$ (icosahedral) entail an enthalpic penalty upon formation of any possible ordered phase. In particular, trying to incorporate either $CB_{11}H_{12}^-$ into an ordered $LiCB_9H_{10}$ or $NaCB_9H_{10}$ lattice[4,16] or $1\text{-}CB_9H_{10}^-$ into an ordered $LiCB_{11}H_{12}$ or $NaCB_{11}H_{12}$ lattice[3] likely leads to some degree of geometric frustration with the surrounding cations. Hence, it appears that the disordered phase is favored outright, in which the exact geometric flavor of orientationally disordered anions is much less important within the more accommodating disordered cation sublattice.

Although solution-drying is likely the preferred route for accomplishing molecular-level mixing of these anions, and past experience indicates that it can also work for synthesizing mixed Li^+ and Na^+ cation phases with *closo*-borate anions,[17] we know that not all such anions can be effectively mixed in this way. For example, our earlier attempts to form a 1:1 solid solution of $Na_2B_{12}H_{12}$ and $Na_2B_{10}H_{10}$ in this way proved to be unsuccessful. One main reason is that each of these fast-ion-conducting compounds can possess varying solubilities and tend to form different stable solid hydrates during precipitation. Upon precipitation, the hydrates of the different compounds often form independently into large crystallites with little mixing. Further vacuum drying leads to coarse mixtures of the original single-anion compounds. Because the anion translational mobilities are extremely low, annealing these coarse mixtures at reasonable temperatures is insufficient to cause molecular-level intermixing of the anions on an acceptable time scale. In these cases, mechanically milling anhydrous compound mixtures is one way to ensure such intimate intermixing, as was demonstrated for a ball-milled 1:1 $Na_2B_{12}H_{12}{:}Na_2B_{10}H_{10}$ mixture,[13] which exhibited a room-temperature bcc-like disordered phase reminiscent of superionic $Na_2B_{12}H_{12}$,[18] but with a smaller unit-cell volume intermediate between those for pure $Na_2B_{12}H_{12}$ and $Na_2B_{10}H_{10}$.

It is worth mentioning that inadvertent yet advantageous anion-mixing effects leading to enhanced cationic conductivity may also be occurring during the alternative solvent-free-synthesis method for producing $B_{12}H_{12}^{2-}$-based compounds via reaction of MH or MBH_4 with $B_{10}H_{14}$.[19,20] It is known that other anions, most notably $B_{10}H_{10}^{2-}$ anions, are routinely present in nontrivial amounts,[19,20] so that the final $M_2B_{12}H_{12}$ may actually be a mixed-anion phase, which based on what we now know, can lead to a solid solution with structural disorder and unexpected conductivity behavior. Indeed, this may explain the much higher room-temperature ionic conductivities observed for $Li_2B_{12}H_{12}$ and the anomalous order–disorder transition temperature observed for $LiNaB_{12}H_{12}$ (with ~14% $B_{10}H_{10}^{2-}$ anions), both compounds which were synthesized by the solvent-free method,[21,22] compared to the corresponding properties for $Li_2B_{12}H_{12}$ and $LiNaB_{12}H_{12}$ samples known to be largely free of such anion impurities.[13,17] From the viewpoint of producing a better ionic conductor, such impurities are desirable and can lead to stabilization of the desired superionic disordered phases at room temperature and below.

We further tested the ball-milling strategy with the present carborate compounds by separately ball-milling 1:1 anhydrous $LiCB_9H_{10}{:}LiCB_{11}H_{12}$ and $NaCB_9H_{10}{:}NaCB_{11}H_{12}$ mixtures. Room-temperature XRPD patterns (Figure S3) confirmed that both ball-milled mixtures formed predominantly hexagonal disordered structures like the pure disordered MCB_9H_{10} compounds (but with slightly expanded unit cells and broadened Bragg peaks), consistent with nanosized crystallites and more complete homogenization. However, annealing these samples for only 1 h at 473 K led to a sharpening of the Bragg peaks presumably due to sintering. The Na-based mixture remained hexagonal, with an XRPD pattern closely resembling that of its solution-dried analog in Figure 1. The Li-based mixture shifted from predominantly hexagonal to a combination of hexagonal and fcc, again with an XRPD pattern closely resembling its solution-dried analog. DSC measurements again showed no phase transitions between 200 and 473 K, and FWSs (Figure S4) indicated anion reorientational mobility behaviors similar to those for the solution-dried samples. Finally, conductivities (Figure S5) followed trends with temperature similar to those of the solution-dried samples, although the values observed for the ball-milled samples (compared to the solution-dried samples) were around 2× larger for Na^+ and 2–7× smaller for Li^+. The reasons for these variations are not yet clear and will require more extensive studies, but they may have something to do with the preparation-dependent differences in particle morphologies, anion mixing, and anion degradations.

Despite these conductivity differences, both methods confirm that anion mixing indeed leads to intimately anion-mixed solid solutions with disordered superionic structures down to subambient temperatures. Further work is in progress to tune the procedures that will yield optimal conductivity properties. Such spectacular mixture-induced behavior is an additional promising development that further enhances the prospects of this broad class of large polyhedral-anion-based compounds for successful incorporation into next-generation, all-solid-state energy-storage devices.

■ EXPERIMENTAL METHODS

Anhydrous lithium and sodium 1-carba-*closo*-decaborates and carba-*closo*-dodecaborates ($LiCB_9H_{10}$, $NaCB_9H_{10}$, $LiCB_{11}H_{12}$, and $NaCB_{11}H_{12}$) were used as starting materials. (N.B., as there are two possible $CB_9H_{10}^-$ isomers, 1-carba- refers to carbon occupying an apical position of the bicapped-square-anti-prismatic $CB_9H_{10}^-$ anion. Here, it is assumed that $CB_9H_{10}^-$ refers to the $1\text{-}CB_9H_{10}^-$ isomer.) Mixed-anion solid-solution phases $Li_2(CB_9H_{10})(CB_{11}H_{12})$ and $Na_2(CB_9H_{10})(CB_{11}H_{12})$ were synthesized by first dissolving equimolar amounts of the respective pure anhydrous components in water followed by solid-hydrate precipitation by room-temperature evacuation of the excess water, and finally by complete removal of any remaining solid-hydrate waters by overnight evacuation at 473 K. For comparison, 100 h ball-milled, 1:1 anhydrous mixtures of $LiCB_9H_{10}{:}LiCB_{11}H_{12}$ and $NaCB_9H_{10}{:}NaCB_{11}H_{12}$ were prepared according to procedures in ref 13. More complete information about starting materials and experimental details concerning XRPD, NMR, DSC, FWSs, and conductivity measurements can be found in the Supporting Information.

Structural depictions were made using the VESTA (Visualization for Electronic and Structural Analysis) software.[23] For all figures, standard uncertainties are commensurate with the observed scatter in the data, if not explicitly designated by vertical error bars.

■ ASSOCIATED CONTENT

■ AUTHOR INFORMATION

Corresponding Authors
*E-mail: wansi.tang@nist.gov.
*E-mail: orimo@imr.tohoku.ac.jp.
*E-mail: udovic@nist.gov.

Notes
The authors declare no competing financial interest.

■ ACKNOWLEDGMENTS

■ REFERENCES

(1) Udovic, T. J.; Matsuo, M.; Unemoto, A.; Verdal, N.; Stavila, V.; Skripov, A. V.; Rush, J. J.; Takamura, H.; Orimo, S. Sodium Superionic Conduction in $Na_2B_{12}H_{12}$. *Chem. Commun.* **2014**, *50*, 3750−3752.

(2) Udovic, T. J.; Matsuo, M.; Tang, W. S.; Wu, H.; Stavila, V.; Soloninin, A. V.; Skoryunov, R. V.; Babanova, O. A.; Skripov, A. V.; Rush, J. J.; et al. Exceptional Superionic Conductivity in Disordered Sodium Decahydro-*Closo*-Decaborate. *Adv. Mater.* **2014**, *26*, 7622−7626.

(3) Tang, W. S.; Unemoto, A.; Zhou, W.; Stavila, V.; Matsuo, M.; Wu, H.; Orimo, S.; Udovic, T. J. Unparalleled Lithium and Sodium Superionic Conduction in Solid Electrolytes with Large Monovalent Cage-like Anions. *Energy Environ. Sci.* **2015**, *8*, 3637−3645.

(4) Tang, W. S.; Matsuo, M.; Wu, H.; Stavila, V.; Zhou, W.; Talin, A. A.; Soloninin, A. V.; Skoryunov, R. V.; Babanova, O. A.; Skripov, A. V.; et al. Liquid-like Ionic Conduction in Solid Lithium and Sodium Monocarba-*Closo*-Decaborates near or at Room Temperature. *Adv. Energy Mater.* **2016**, *6*, 1502237.

(5) Kamaya, N.; Homma, K.; Yamakawa, Y.; Hirayama, M.; Kanno, R.; Yonemura, M.; Kamiyama, T.; Kato, Y.; Hama, S.; Kawamoto, K.; et al. A Lithium Superionic Conductor. *Nat. Mater.* **2011**, *10*, 682−686.

(6) Sadikin, Y.; Brighi, M.; Schouwink, P.; Černý, R. Superionic Conduction of Sodium and Lithium in Anion-Mixed Hydroborates $Na_3BH_4B_{12}H_{12}$ and $(Li_{0.7}Na_{0.3})_3BH_4B_{12}H_{12}$. *Adv. Energy Mater.* **2015**, *5*, 1501016.

(7) Zhang, L.; Yang, K.; Mi, J.; Lu, L.; Zhao, L.; Wang, L.; Li, Y.; Zeng, H. Na_3PSe_4: A Novel Chalcogenide Solid Electrolyte with High Ionic Conductivity. *Adv. Energy Mater.* **2015**, *5*, 1501294.

(8) Monti, D.; Jónsson, E.; Palacín, M. R.; Johansson, P. Ionic Liquid Based Electrolytes for Sodium-Ion Batteries: Na^+ Solvation and Ionic Conductivity. *J. Power Sources* **2014**, *245*, 630−636.

(9) Ding, M. S.; Xu, K.; Zhang, S. S.; Amine, K.; Henriksen, G. L.; Jow, T. R. Change of Conductivity with Salt Content, Solvent Composition, and Temperature for Electrolytes of $LiPF_6$ in Ethylene Carbonate-Ethyl Methyl Carbonate. *J. Electrochem. Soc.* **2001**, *148*, A1196−A1204.

(10) Kalhoff, J.; Eshetu, G. G.; Bresser, D.; Passerini, S. Safer Electrolytes for Lithium-Ion Batteries: State of the Art and Perspectives. *ChemSusChem* **2015**, *8*, 2154−2175.

(11) Lipscomb, W. H. *Boron Hydrides*; W. A. Benjamin, Inc.: New York, 1963.

(12) Wang, Y.; Richards, W. D.; Ong, S. P.; Miara, L. J.; Kim, J. C.; Mo, Y.; Ceder, G. Design Principles for Solid-State Lithium Superionic Conductors. *Nat. Mater.* **2015**, *14*, 1026−1031.

(13) Tang, W. S.; Matsuo, M.; Wu, H.; Stavila, V.; Unemoto, A.; Orimo, S.; Udovic, T. J. Stabilizing Lithium and Sodium Fast-Ion Conduction in Solid Polyhedral-Borate Salts at Device-Relevant Temperatures. *Energy Storage Mater.* **2016**, *4*, 79−83.

(14) Skripov, A. V.; Skoryunov, R. V.; Soloninin, A. V.; Babanova, O. A.; Tang, W. S.; Stavila, V.; Udovic, T. J. Anion Reorientations and Cation Diffusion in $LiCB_{11}H_{12}$ and $NaCB_{11}H_{12}$: ^{1}H, ^{7}Li, and ^{23}Na NMR Studies. *J. Phys. Chem. C* **2015**, *119*, 26912−26918.

(15) Markert, J. T.; Cotts, E. J.; Cotts, R. M. Hydrogen Diffusion in the Metallic Glass a-$Zr_3RhH_{3.5}$. *Phys. Rev. B: Condens. Matter Mater. Phys.* **1988**, *37*, 6446−6452.

(16) Wu, H.; Tang, W. S.; Zhou, W.; Tarver, J. D.; Stavila, V.; Brown, C. M.; Udovic, T. J. The Low-Temperature Structural Behavior of Sodium 1-Carba-Closo-Decaborate: $NaCB_9H_{10}$. *J. Solid State Chem.* **2016**, *243*, 162−167.

(17) Tang, W. S.; Udovic, T. J.; Stavila, V. Altering the Structural Properties of $A_2B_{12}H_{12}$ Compounds via Cation and Anion Modifications. *J. Alloys Compd.* **2015**, *645*, S200−S204.

(18) Verdal, N.; Her, J.-H.; Stavila, V.; Soloninin, A. V.; Babanova, O. A.; Skripov, A. V.; Udovic, T. J.; Rush, J. J. High-Temperature Phase Transitions in $Li_2B_{12}H_{12}$ and $Na_2B_{12}H_{12}$. *J. Solid State Chem.* **2014**, *212*, 81−91.

(19) Sivaev, I. B.; Bregadze, V. I.; Sjöberg, S. Chemistry of *Closo*-Dodecaborate Anion $[B_{12}H_{12}]^{2−}$: A Review. *Collect. Czech. Chem. Commun.* **2002**, *67*, 679−727.

(20) He, L.; Li, H.-W.; Hwang, S.-J.; Akiba, E. Facile Solvent-Free Synthesis of Anhydrous Alkali Metal Dodecaborate $M_2B_{12}H_{12}$ (M = Li, Na, K). *J. Phys. Chem. C* **2014**, *118*, 6084−6089.

(21) Teprovich, J. A., Jr.; Colón-Mercado, H.; Washington, A. L., II; Ward, P. A.; Greenway, S.; Missimer, D. M.; Hartman, H.; Velten, J.; Christian, J. H.; Zidan, R. Bi-functional $Li_2B_{12}H_{12}$ for Energy Storage and Conversion Applications: Solid-State Electrolyte and Luminescent Down-Conversion Dye. *J. Mater. Chem. A* **2015**, *3*, 22853−22859.

(22) He, L.; Li, H.-W.; Nakajima, H.; Tumanov, N.; Filinchuk, Y.; Hwang, S.-J.; Sharma, M.; Hagemann, H.; Akiba, E. Synthesis of a Bimetallic Dodecaborate $LiNaB_{12}H_{12}$ with Outstanding Superionic Conductivity. *Chem. Mater.* **2015**, *27*, 5483−5486.

(23) Momma, K.; Izumi, F. *VESTA 3* for Three-Dimensional Visualization of Crystal, Volumetric and Morphology Data. *J. Appl. Crystallogr.* **2011**, *44*, 1272−1276.